International Journal of Multiphase Flow 35 (2009) 129–141

Contents lists available at ScienceDirect

International Journal of Multiphase Flow

journal homepage: www.elsevier.com/locate/ijmulflow

Numerical simulation of the Reynolds number effect on gas-phase turbulence modulation

Kunn Hadinoto [a,*], Jennifer Sinclair Curtis [b]

[a] School of Chemical and Biomedical Engineering, Nanyang Technological University, Singapore 637459, Singapore
[b] Department of Chemical Engineering, University of Florida, Gainesville, FL 32611, USA

ARTICLE INFO

Article history:
Received 14 May 2008
Received in revised form 6 October 2008
Accepted 10 October 2008
Available online 21 October 2008

ABSTRACT

The enhancement of the gas-phase turbulence intensity at high Reynolds number (Re) has been observed experimentally by Hadinoto et al., in dilute-phase particle-laden flows of non-massive particles ($\leqslant 200$ μm). This work attempts to assess the predictive capability of a two-phase flow computational fluid dynamics (CFD) model, which is based on the kinetic theory of granular flow, in capturing the trend in the gas-phase turbulence modulation as a function of Re. In addition, the model predictive capability in simulating gas-particle flow regime of moderate Stokes number (St_T) and low Re is examined. The use of different drag correlations and turbulence closure models is explored for this purpose. The simulation results suggest that the current state of the two-phase flow CFD model is not yet capable of accurately predicting the Re dependence of the gas-phase turbulence modulation. The two-phase flow CFD model, however, is more than capable in yielding good predictions at both the mean and fluctuating velocity levels for the case where the turbulence enhancement at high Re is not evident.

1. Introduction

Processes involving turbulent particle-laden flows are widely encountered in the industry, such as in fluid catalytic cracking reactors, coal gasifiers, pneumatic conveying systems, and pharmaceutical batch crystallizers. A majority of these processes, however, do not operate at their optimal condition due to a lack of understanding in the particulate flow behavior during the process design stage. Design, optimization, and scale-up of these processes require a reliable computational fluid dynamics (CFD) simulation tool that can accurately capture the intricate particle-laden flow phenomena. Significantly, a case study on the economic impact of employing CFD simulation in the chemical industry suggests that the achieved economical benefits generate a sixfold return on the total investment required to implement the CFD (Davidson, 2001).

Unfortunately, as opposed to the single-phase flow modeling, the current state of two-phase flow CFD model is not yet capable of accurately predicting the multiscale flow phenomena in particle-laden flows, hence continuous advancement of the two-phase flow CFD model is critical. In conjunction with the modeling work, non-intrusive flow measurements, where multiple flow variables are measured simultaneously, are needed to validate the CFD model prediction. The present investigation focuses on dilute-phase gas–particle pipe flows, which represent particle-laden flows in a pneumatic conveying system.

One flow phenomenon of primary interest is the effect of Reynolds number (Re) variation on the gas-phase turbulence modulation. The gas-phase turbulence intensity has a direct impact on the pressure drop (i.e. energy requirement) and heat/mass transfer rates in the conveying line. The Re influence on the gas-phase turbulence intensity is of significant practical importance as changes in process design parameters (e.g. flow geometry, flow capacity, and fluid property), during scale-up or debottlenecking, must lead to a Re variation. In the present work, the CFD model ability in predicting the trends in the Re dependence of the gas-phase turbulence modulation, which were obtained experimentally by Hadinoto et al. (2005), is examined.

The presence of the particles can either attenuate or enhance the fluid-phase turbulence intensity with respect to its unladen value. The turbulence modulation can be attributed to (1) fluid–particle interactions, which are significant when particle volume fraction, υ, is larger than 10^{-6} (Elghobashi, 1994) and (2) interparticle collisions that lead to a redistribution of the particle fluctuating velocity, which in turn induces disturbances in the fluid flow field. Importantly, the modulated fluid-phase turbulence in turn influences the particle fluctuating motion by means of the fluctuating drag force resulting in a two-way coupling interaction between the two phases.

Significantly, the two-way coupling interaction between the fluid-phase turbulence and particle fluctuation has been found to influence the pressure drop in the conveying line. Gas-phase turbulence enhancement in the presence of massive particles ($d_p > 4$ mm) was found to lead to an increased pressure drop (Vasquez et al., 2008), whereas gas-phase turbulence attenuation

* Corresponding author. Tel.: +65 6514 8381; fax: +65 6794 7553.
E-mail address: kunnong@ntu.edu.sg (K. Hadinoto).

0301-9322/$ - see front matter © 2008 Elsevier Ltd. All rights reserved.
doi:10.1016/j.ijmultiphaseflow.2008.10.003

in the presence of fine particles (d_p < 75 μm) was found to result in a decreased pressure drop (Marcus et al., 1990).

Hadinoto (2004) and Hadinoto et al. (2005) conducted experimental studies to explore the effect of Re variation on the gas-phase turbulence modulation in a dilute-phase pneumatic conveying system. The Reynolds number is defined as $\mathrm{Re} = 2\rho_f U_{sf} R/\mu_f$, where R is the pipe radius, ρ_f is the gas density, U_{sf} and μ_f are the mean superficial velocity and gas viscosity, respectively. Their experiments were conducted in a vertically downward pipe flow using high-density glass bead particles ($\rho_s = 2500\ \mathrm{kg/m^3}$) and low-density cenospheres particles ($\rho_s = 700\ \mathrm{kg/m^3}$) of various sizes ($60 \leqslant d_p \leqslant 200$ μm). The effect of particle loading, m, which was defined as the ratio of the particle mass flow rate to that of the gas, was also investigated for $0.4 \leqslant m \leqslant 4.0$. They varied Re between $6000 \leqslant \mathrm{Re} \leqslant 24,000$ by changing the transport velocity (i.e. mean superficial velocity), while maintaining other parameters (e.g. particle loading, size, and density) constant.

At low particle loadings ($m \leqslant 1.0$), Hadinoto et al. (2005) reported that the gas-phase turbulence intensity in the pipe core increased with increasing Re. The trend was thus in contrast to that of the unladen flow in which the turbulence intensity decreased with Re as $\propto 0.16\mathrm{Re}^{-1/8}$ (Kiml et al., 2004). In the presence of the 200-μm glass bead particles at $m = 0.7$, the turbulence intensity in the pipe core for all Re investigated was enhanced with respect to the unladen flow at the same Re, as indicated by the positive values in the difference between the laden and unladen turbulence intensities (Fig. 1). Importantly, the degree of the turbulence enhancement was intensified with increasing Re, as a result of an increased magnitude of the turbulence intensity, and not due to the decreasing turbulence intensity of the unladen flow at higher Re. A similar trend was observed by Hadinoto (2004) in the presence of the 70-μm glass bead particles at $m = 0.4$ (Fig. 2). The gas-phase turbulence intensity in the pipe core, which was initially attenuated with respect to the unladen flow at Re = 6000, became enhanced when Re was raised to 13,000.

The primary aim of this work is to examine whether the trend in the gas-phase turbulence modulation as a function of Re can be captured by the existing two-phase flow CFD model. The total number of particles typically present in particle-laden flows of practical interest, even in dilute phase flows ($\upsilon < 10^{-3}$), is extremely large. Hence, it is impractical to solve for the motion of each particle through Lagrangian or discrete element methods. Consequently, particle-laden flows in industrial-scale processes are typically simulated in commercial CFD software (e.g. Fluent, CFX) using continuum-based two-fluid models (i.e. Eulerian model).

In turbulent particle-laden flow simulations, the two-fluid CFD modeling framework has already successfully demonstrated its capability in predicting pressure drop, mean phase velocities, and macroscale particle-laden flow phenomena, such as choking and segregation. For that reason, a two-fluid CFD model developed by Hadinoto and Curtis (2004) is employed in the present work. Their model treated the particle phase as a continuum and employed the kinetic theory of granular flow concept to describe the particle-phase stresses. The kinetic theory concept has been widely implemented in the modeling of collision-dominated particle-laden flows, such as in dilute-phase pneumatic conveying and circulating fluidized bed. Collision-dominated flows are typically characterized by their high particle Stokes number, $St_T \gg 1$ (Eq. (1)).

$$St_T = \frac{\rho_s d_p \sqrt{T}}{9\mu_f} \tag{1}$$

where ρ_s is the particle density, and T is the granular temperature, which is defined as $T = \frac{1}{3}\overline{u'_{si}u'_{si}}$ and u'_{si} is the particle fluctuating velocity.

For such flows, particle concentration is sufficiently high to allow inelastic interparticle collisions to occur readily and rapidly, such that particle fluctuating motion is governed by the interparticle collisions, and not by their interactions with the small-scale turbulent eddies. The particles, however, remain dispersed in a turbulent fluid flow field having a finite fluid inertia, as characterized by its microscale Reynolds number, Re_T, that is larger than one (Eq. (2)).

$$\mathrm{Re}_T = \frac{\rho_f d_p \sqrt{T}}{\mu_f} \tag{2}$$

As $\mathrm{Re}_T \geqslant 1$, the impact of the fluid turbulence on the particle fluctuating motion through hydrodynamic interactions (i.e. fluctuating viscous drag force) cannot be neglected.

Unfortunately, exact descriptions for the hydrodynamic interactions do not exist, hence empirical closure models are often required to describe fluid–particle interaction mechanisms, such as fluctuating drag force and particle wake formation for high Re_P flows, where $\mathrm{Re}_P = \rho_f d_p |U_f - U_s|/\mu_f$. Due to their empirical nature,

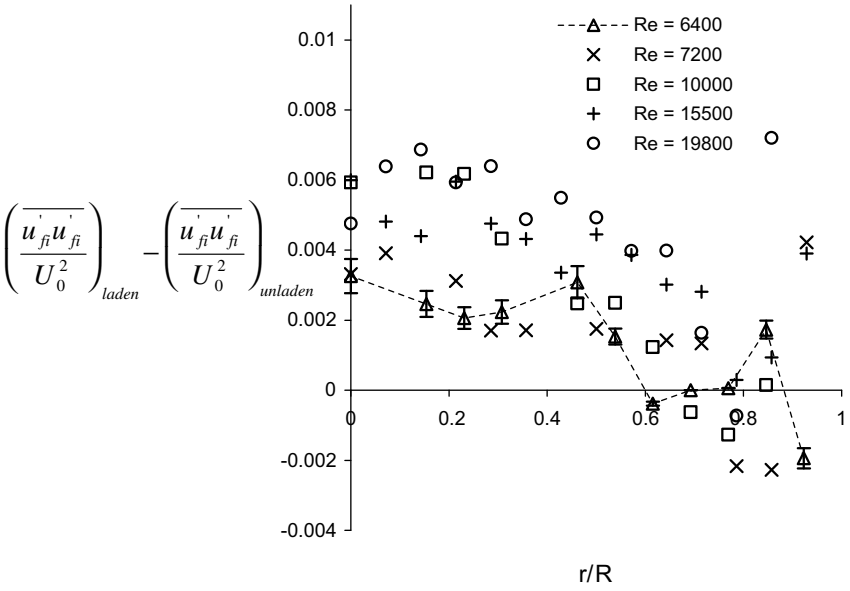

Fig. 1. The degree of the gas-phase turbulence modulation as a function of the Re in the presence of the 200 μm glass beads at $m = 0.7$ (data of Hadinoto et al., 2005).

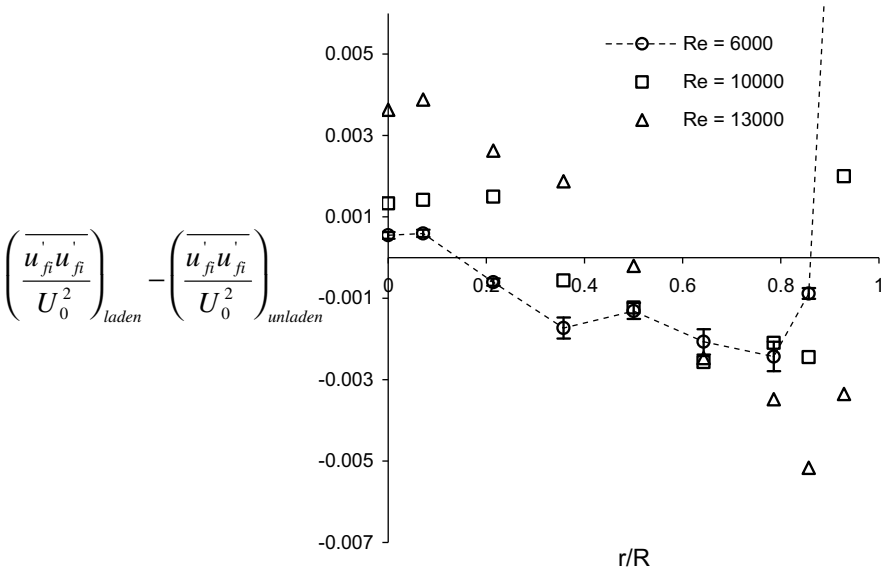

Fig. 2. The degree of the gas-phase turbulence modulation as a function of the Re in the presence of the 70 μm glass beads at $m = 0.4$ (data of Hadinoto, 2004).

none of the closure models currently available in the literature is capable of accurately predicting the turbulence modulation and particle fluctuation for different particle-laden flow regimes. For that reason, numerical results obtained from the Lagrangian, discrete element, and direct numerical simulation methods have been implemented into the two-fluid modeling framework, so that the hydrodynamic interactions can be more accurately described. Unfortunately, the high-computational cost demanded by these methods limits the simulations to low-Re turbulent flows at extremely dilute particle concentrations, which lack industrial relevance. As a result, the two-fluid CFD model is still the preferred method in simulations of large-scale processes despite its shortcomings.

For collision-dominated particle-laden flows, the current state of the two-fluid CFD model exhibits a good predictive capability for flows in which the ratio of the particle inertia to the fluid inertia is large ($\gg 1$), where the kinetic theory of granular flow concept is highly applicable. An example of such flows is a rapid flow of high-inertia particles ($d_p > 200$ μm, $\rho_s/\rho_f \gg 1$) in gas. A majority of the two-fluid CFD models available in the literature (e.g. Hadinoto and Curtis (2004), Bolio et al. (1995), Zhang and Reese (2003a)), and commercially available models (e.g. Fluent, CFX) have been successfully validated at both the mean and fluctuating velocity levels using experimental data of rapid gas flows of massive particles (e.g. Lee and Durst (1982), Tsuji et al. (1984)).

The model predictive capability, however, has not been thoroughly examined for (1) particle-laden flows involving lower inertia particles (e.g. small size, low density, high porosity) and for (2) slow-moving particle-laden flows (i.e. low-Re turbulent flows). In that regard, the Hadinoto and Curtis (2004) model was reported to overpredict the pressure drop in the pneumatic conveying of 70 μm glass bead particles, whereas more accurate predictions were obtained for the higher-inertia 200 and 500 μm particles (Henthorn et al., 2005). On a similar note, simulation of a dilute-phase circulating fluidized bed using Fluent yielded worse predictions for the granular temperature for operations at lower transport velocities (Vaishali et al., 2007).

Therefore, in conjunction to our investigation on the Re dependence of the turbulence modulation, the present work also intends to evaluate the model predictive capability for gas–particle flow systems in which low-inertia particles and low-Re turbulent flows are involved. The model predictions are compared with the experimental data of (Hadinoto, 2004), which encompass a wide Re range (Table 1), as opposed to previous studies that were limited to data of rapid flows of high-inertia particles. The emphasis is placed on the model ability to predict the mean velocities, the gas-phase turbulent kinetic energy, and the granular temperature. For that purpose, the use of different drag correlations and turbulence closure models is explored. To summarize, the objectives of the present work are (1) to assess the CFD model predictive capability in capturing the trend in the gas-phase turbulence modulation as a function of Re and (2) to examine its predictive capability for low-Re turbulent particle-laden flows involving low to moderate-inertia particles.

2. Two-phase flow CFD modeling efforts

The framework of the two-fluid CFD model employed in the present work was developed by Hadinoto and Curtis (2004). The descriptions of the drag correlations and fluctuating energy balances have been slightly modified here. The simulation is conducted for a steady state, fully-developed gas–particle flow in a vertical downward pipe, which corresponds to the experimental flow configuration of Hadinoto (2004). The particles are assumed to be spherical, non-cohesive, frictionless, and monodisperse in size. In the two-fluid model, the inelasticity of the interparticle collisions is characterized by the coefficient of restitution, e, which is defined as the ratio of the particle rebound velocity to the particle impact velocity. A value of $e \approx 1$ indicates a perfectly elastic collision in vacuum.

When two particles collide in fluid, the particle fluctuating energy is dissipated into (1) the thermal heat due to the inelasticity, and into (2) the fluid fluctuation as the particles must exert work

Table 1
Summary of the experimental case studies – data of Hadinoto (2004).

Particle	ρ_s (kg/m^3)	m	Re	St_T	Re_T	Re_P
Case 1: Glass beads 70 μm	2500	0.4	6000	507	2.2	10
			10,000	946	4.0	13
			13,000	1250	5.3	19
Case 2: Cenospheres 60 μm	700	0.4	6000	126	1.9	3
			10,000	219	3.3	5
			13,000	302	4.6	7

on the fluid to displace the interstitial fluid between the two particle surfaces (i.e. lubrication effect). As a result, two distinct coefficients of restitution, e_s and e_f, where $e_f \leqslant e_s$, are employed to characterize the inelasticity of interparticle collisions in vacuum and fluid, respectively. The importance of the lubrication effect in the interparticle collisions is characterized by the ratio e_f/e_s, which is a function of St_T. A master plot of the ratio e_f/e_s versus St_T has been obtained experimentally for a wide range of particle-laden flow systems (Gondret et al., 2002).

Their experimental results suggested that the lubrication effect was most significant for interparticle collisions in a highly viscous fluid, as characterized by the low St_T (e.g. slow liquid–particle flow). Consequently, the lubrication effect in gas–particle flows is significant only for lower St_T flows, which occur when (1) the particle density or size is reduced, hence the particle inertia is reduced or when (2) the particle impact velocity is reduced by lowering the mean shear-force exerted by the fluid (i.e. lower fluid mean velocity). In this work, St_T of the two case studies investigated vary from 100 to 1300 (Table 1). According to the master plot of Gondret et al. (2002), the ratio of e_f/e_s varies from about 0.6 at $St_T \approx 100$ to 0.8 at $St_T \approx 500$, and 0.9 at $St_T \approx 1000$, whereas the ratio e_f/e_s is essentially one for $St_T \geqslant 1300$. Therefore, the lubrication effect is significant for the flows involving the cenospheres particles due to their lower particle density.

The low particle loading in the two case studies, however, indicates that the contribution from the interparticle collisions in the particle fluctuating energy balance would relatively be small, though not negligible, compared with the contributions from the particle-phase stresses and hydrodynamic interactions. As a result, even though the lubrication effect is physically important, its impact on the resulting model predictions may not be significant at this low particle loading. Nevertheless, the present model has incorporated the lubrication effect into its formulation.

2.1. Governing equations

For a steady-state fully developed pipe flow, the governing equations for the particle phase comprise of the continuity equation, the axial and radial momentum balances, and the particle fluctuating energy balance. The governing equations for the fluid phase are reduced to the continuity equation, the axial momentum balance, and the turbulent kinetic energy balance. The detailed formulations of these equations have been provided in Hadinoto and Curtis (2004), and not repeated here, except for the particle fluctuating energy and fluid turbulent kinetic energy balances, where modifications have been made.

The balance for the particle fluctuating energy (i.e. granular temperature) is formulated as follow:

$$0 = \underset{(a)}{-\frac{1}{r}\frac{\partial}{\partial r}(rq_{PTr})} \underset{(b)}{-\sigma_{rz}\frac{\partial U_{sz}}{\partial r}} \underset{(c)}{-\gamma} \underset{(d)}{-3\beta T} \underset{(e)}{+\beta\overline{u_{si}'u_{fi}'}} \tag{3}$$

The first three terms on the right-hand side of Eq. (5), respectively, represent (a) diffusion of the granular temperature due to local temperature gradients, (b) generation due to the mean shear flow, and (c) dissipation due to the inelastic interparticle collisions, which includes the losses to the thermal heat and fluid fluctuations. The detailed descriptions of the particle-phase stresses (q_{PTr}, σ_{rz}) and viscosity have been provided in Hadinoto and Curtis (2004).

The last two terms, (d) and (e), represent the fluid–particle interactions at the fluctuating velocity level (i.e. hydrodynamic interactions), where β is the drag coefficient, and u_{fi}', u_{si}' are the fluid and particle fluctuating velocities, respectively. The fourth term (d) corresponds to a sink of the granular temperature due the fluctuating viscous drag force. The fifth term (e) corresponds to a source of the granular temperature due to long-range fluid–particle interactions (Koch, 1990), where disturbance in the fluid turbulent flow field induced by the fluctuating motion of the neighboring particles enhances the particle fluctuating motion.

The balance for the fluid turbulent kinetic energy, $k = \frac{1}{2}\overline{u_{fi}'u_{fi}'}$, where u_{fi}' is the fluid fluctuating velocity, is based on the low-Re k–ε turbulence model (Myong and Kasagi, 1990) and formulated as follows:

$$0 = \underset{(a)}{\frac{1}{r}\frac{\partial}{\partial r}\left[r(1-\upsilon)\left(\mu_{ef} + \frac{\mu_T}{\sigma_k}\right)\frac{\partial k}{\partial r}\right]} + \underset{(b)}{(1-\upsilon)\mu_T\left(\frac{\partial U_{fz}}{\partial r}\right)^2} \underset{(c)}{-\rho_f(1-\upsilon)\varepsilon} + \underset{(d)}{\frac{\eta_s - \eta_f}{\eta_f}\mu_s^* G_{1c}\frac{\partial U_{sz}}{\partial r}\frac{\partial U_{fz}}{\partial r}} \underset{(e)}{+\gamma_{FKET}} \underset{(f)}{-2\beta k} \underset{(g)}{+\beta\overline{u_{si}'u_{fi}'}} \underset{(h)}{+\overline{E_W}} \tag{4}$$

where $\mu_{ef}, \mu_T, \sigma_k$ and μ_s^* are the effective fluid viscosity, the eddy viscosity, turbulent Prandtl number, and the particle-phase viscosity, respectively, and $\eta = (1+e)/2$. The first three terms on the right-hand side of Eq. (3) are (a) diffusion due to local turbulent energy gradients, (b) generation due to the mean shear flow, and (c) viscous dissipation, ε, of the fluid turbulent kinetic energy, respectively.

The fourth and fifth terms, (d) and (e), represent sources of turbulent kinetic energy due to inelastic interparticle collisions, which exist only when the lubrication effect is significant ($e_f < e_s$). The fourth term (d) is a source of turbulent kinetic energy generated by the collisional fluid stress (G_{1c}), whereas the fifth term (e) is a source due to the lubrication effect in which the particle fluctuating energy is dissipated into the fluid fluctuation. The mathematical description for γ_{FKET}, which can be derived from the definitions of e_s and e_f, is presented as:

$$\gamma_{FKET} = \left(\frac{e_s^2 - e_f^2}{1 - e_f^2}\right)\gamma \tag{5}$$

where the multiplying factor in front of γ denotes a fraction of the particle fluctuating energy that is dissipated into the fluid fluctuation in the interparticle collisions.

The sixth and seventh terms, (f) and (g), correspond to the fluid–particle interactions at the fluctuating velocity level, where (f) represents a sink term due the fluctuating viscous drag force, and (g) represents a source term due to the abovementioned long-range fluid–particle interaction. Finally, the last term (h) corresponds to a turbulent kinetic energy generation as a result of the wake generated behind the particles ($\overline{E_W}$), which becomes significant for flows with $Re_P \geqslant 400$ (Hetsroni, 1989). As the present investigation involves flows with very low Re_P (<20, Table 1), this turbulence generation mechanism is set to zero in the simulation.

2.2. Model solution

Governing equations describing the relationship between U_{fz}, U_{sz}, T, k, ε, and υ are solved in conjunction with their boundary conditions. At the pipe center, symmetry requires that the gradients of all the six variables to be zero. At the pipe wall, no-slip boundary conditions are enforced for the fluid phase (U_{fz}, k, ε), whereas the boundary conditions of the particle phase follow the formulations by (Johnson and Jackson, 1987). The equations are solved using an adaptation of the implicit finite volume marching technique by (Patankar, 1980). In this technique, the problem is formulated as pseudo-transient and is integrated in time until a steady-state solution is obtained. The model requires initial estimates for the pressure drop and the centerline particle volume fraction. These two parameters are iterated until the target values for the particle loading and the fluid centerline mean velocity are achieved.

For the glass bead particles, the values of the coefficients of restitution for the interparticle collisions (e_s) and particle–wall collisions (e_{ws}) in vacuum are obtained from Goldsmith (1960). The value of e_s for the cenospheres particles is estimated to be equal to that of the glass bead particles, as experimental data for the cenospheres particles are not available. The value of e_{ws} for the cenospheres particles, on the other hand, is obtained by selecting an e_{ws} value that ensures the predicted granular temperature adjacent to the pipe wall agrees with the experimental value at one flow condition. The selected e_{ws} value is subsequently employed for simulations at different flow conditions, therefore, e_{ws} is not employed as a tuning parameter. Next, the corresponding coefficient of restitution values for collisions in fluid (e_f and e_{wf}) are extracted from the abovementioned master plot of e_f/e_s versus St_T (Table 2).

In addition, the boundary conditions of Johnson and Jackson (1987) necessitate a specification for the specularity coefficient, σ, which represents the fraction of the particle tangential momentum that is lost in particle–wall collisions. The value of σ varies from 0 to 1 for smooth to rough wall surfaces, respectively. The specularity coefficient is important because it influences the mean slip velocity and the particle fluctuating velocity predictions near the pipe wall. In this work, σ is selected for one experimental condition by matching the predicted particle slip velocity near the pipe wall with the experimental value. The σ value obtained by this procedure is employed for the subsequent simulations at different flow conditions (Table 2). Therefore, this work does not employ either σ or e_{ws} as a tuning parameter to improve the model predictive capability.

2.3. Selection of drag correlations

In dilute-phase particle-laden flows, the hydrodynamic interactions are often as influential as the interparticle collisions, if not more, in dictating the particle fluctuating motion and the resulting fluid-phase turbulence modulation. The importance of the hydrodynamic interactions becomes more evident for low-inertia particles, which are more responsive to the change in the fluid fluctuation than their high-inertia particles counterparts. Therefore, accurate descriptions of the hydrodynamic interactions are particularly essential in the simulations of moderate St_T flows ($100 \leqslant St_T \leqslant 500$), which are apparent in this work, particularly for flows involving the cenospheres particles.

Hadinoto and Curtis (2004) reported that the granular temperature was often overpredicted for non-massive particles ($d_p < 200$ μm). The overprediction of the granular temperature in turn negatively affected the turbulent kinetic energy prediction, thereby the pressure drop prediction. They initially thought that the overpredicted granular temperature was resulted from the omission of the lubrication effect in the model formulation. Incorporating the lubrication effect indeed resulted in a significant improvement in the granular temperature prediction for turbulent liquid-particle flows. In gas-particle flows, however, they found that the improvement was apparent only at high particle loadings ($m > 1$) in which interparticle collisions were significant.

Table 2
Summary of the model parameters for Cases 1 and 2.

Particle	Re	e_s	e_{ws}	e_f	e_{wf}	σ
Case 1: Glass beads $m = 0.4$	6000	0.94	0.15	0.85	0.13	0.008
	10,000			0.90	0.14	
	13,000			0.94	0.15	
Case 2: Cenospheres $m = 0.4$	6000	0.94	0.94	0.75	0.75	0.008
	10,000			0.80	0.80	
	13,000			0.85	0.85	

For gas-particle flows at low particle loadings apparent in the present work, the results of our preliminary study suggest that incorporating the lubrication effect leads only to a minor improvement (<8%) in the granular temperature prediction. As a result, the particle fluctuating intensity remains overpredicted. A closer look on the energy budgets of the particle fluctuating energy balance (Eq. (5)) reveals that the collisional contribution (γ) at low particle loadings is very small relative to the other contributions. In term of their magnitude, the significant contributions are (1) the particle-phase stresses derived from the kinetic theory of granular flow, which have been extensively verified and (2) the hydrodynamic interactions that are described using empirical drag correlations and turbulence closure models for $\overline{u'_{si}u'_{fi}}$. Consequently, the choices of the drag correlations and closure models have a major impact on the resulting granular temperature prediction.

Most drag correlations reported in the literature (e.g. Richardson and Zaki (1954), Wen and Yu (1966), Ding and Gidaspow (1990), Difelice (1994)) were derived from liquid–particle flow data. These empirical drag correlations were based on experimental data of sedimentation, bed expansion, and pressure drop measurement in liquid-phase fluidized or fixed beds. These correlations were then extrapolated to gas–particle flow systems, and have been widely adopted in gas–particle flow modeling. Their applicability to gas–particle flows has been examined at the mean level predictions (i.e. mean velocity, volume fraction, and pressure drop), but not at the fluctuating velocity level.

Yasuna et al. (1995) reported that the model predictions of the mean velocity, pressure drop, and particle volume fraction were insensitive to the choice of the drag correlation. Importantly, Du et al. (2006) reported that the effects of employing different drag correlations on the mean level predictions in a gas-phase fluidized bed were significant only at high particle concentrations ($\upsilon > 10^{-1}$). In general, the Ding and Gidaspow (1990) drag correlation has been most widely used in gas–particle flow modeling. It has been implemented by a majority of the two-fluid CFD models available in the literature (e.g. Agrawal et al. (2001), Zhang and Reese (2003a), Hadinoto and Curtis (2004)). The decision to employ the Ding and Gidaspow (1990) correlation, however, is largely based on the comparison at the mean level predictions. Whether a similar decision should be made at the fluctuating velocity level merits a further investigation.

In that regard, new drag correlations derived from gas–particle flow data have recently emerged in the literature (e.g. Makkawi and Wright (2003), Mabrouk et al. (2007)). In addition, Louge et al. (1991) and Zhang and Reese (2003b) proposed to incorporate the fluctuating nature of the particle motion in calculating the slip velocity, as opposed to using the time-averaged velocity. They reported a notable improvement in the pressure drop prediction when this effect was incorporated into the Wen and Yu (1966) correlation. Furthermore, a new drag correlation obtained from the lattice Boltzmann simulation of gas flowing through a fixed array of particles has been reported by Hill et al. (2001). Their drag correlation can potentially be applicable to gas-particle flows at very high St_T and low Re_T. For such flows, the particle translates through the fluid with a negligible change in its velocity in response to the viscous drag force. As a result, the hydrodynamic interactions for these particles resemble those stationary particles in a fixed-array system.

In the wake of these new developments, the present work attempts to evaluate the impacts of employing the new drag correlations on the model predictions, particularly for moderate St_T flows. An emphasis is placed on the predictions at the fluctuating velocity level (i.e. gas-phase turbulent kinetic energy and granular temperature). Table 3 summarizes the seven drag correlations investigated in the present work, which include (1) the newly-developed correlations from the lattice Boltzmann simulation of Hill et al. (2001),

Table 3
Summary of drag correlations.

$F_{drag}=\beta(U_{fz}-U_{sz})$

$\beta=\frac{3}{4}\frac{\rho_f}{d_p}C_D\upsilon|U_{fz}-U_{sz}|f(\upsilon)$

$Re_P^*=\frac{(1-\upsilon)\rho_f d_p|U_{fz}-U_{sz}|}{\mu_f}$

Drag correlation	C_D	$f(\upsilon)$
Ding and Gidaspow (1990)	$\frac{24}{Re_p^*}\left(1+0.15Re_p^{*0.687}\right)$	$(1-\upsilon)^{-2.65}$
Arastoopour et al (1990)	$\frac{4}{3}(\frac{17.3}{Re_p^*}+0.336)$	$(1-\upsilon)^{-2.80}$
Nieuwland et al (1994)	$\frac{24}{Re_p^*}\left(1+0.15Re_p^{*0.687}\right)$	$(0.997+442.4\upsilon-1733.4\upsilon^2)^{-1}$
Difelice(1994)	$\left(0.63+\frac{4.8}{\sqrt{Re_p^*}}\right)^2$	$3.7-0.65\exp[-\frac{1}{2}(1.5-Log Re_p^*)^2]$
Makkawi and Wright (2003)	$3+303\exp(-0.135Re_p^*)$	1
Hill et al(2001)		$F_{drag}=\frac{18\mu_f\upsilon}{d_p^2}(U_{fz}-U_{sz})f(\upsilon)$ $\quad Re_P<20$
		$f=f_0+f_1Re_P^2/4$
		$f_0=\frac{1+3(\upsilon/2)^{0.5}+135/64\upsilon\ln\upsilon+16.14\upsilon}{1+0.681\upsilon-8.48\upsilon^2+8.16\upsilon^3}$ $\quad \upsilon<0.4$
		$f_1=\frac{\sqrt{2}}{40\sqrt{\upsilon}}-0.182+1.01\sqrt{\upsilon}$ $\quad \upsilon<0.03$
Zhang and Reese (2003b)		$\beta=\frac{3}{4}\frac{\rho_f}{d_p}C_D\upsilon[(U_{fz}-U_{sz})^2+\frac{8T}{\pi}]^{0.5}(1-\upsilon)^{-2.65}$ C_D follows Ding and Gidaspow (1990)

(2) from the gas fluidized bed data of Makkawi and Wright (2003), and (3) existing correlations that were derived from various fixed-bed and sedimentation flow data, which are notably distinct from the Ding and Gidaspow (1990) correlation (i.e. Arastoopour et al. (1990), Nieuwland et al. (1994), Difelice (1994)). In addition, the effect of incorporating the particle fluctuating velocity into the slip velocity calculation ($U_{Slip}=\sqrt{(U_{fz}-U_{sz})^2+8T/\pi}$), as proposed by Zhang and Reese (2003b), is also examined.

2.4. Selection of turbulence closure models

Besides the drag correlation, the descriptions for the hydrodynamic interactions require a turbulence closure model for the $\overline{u'_{si}u'_{fi}}$ correlation, which determines the magnitude of the long-range fluid–particle interaction. Determination of the closure model for the $\overline{u'_{si}u'_{fi}}$ correlation is a very challenging task as an experimental technique that is capable of simultaneously acquiring the fluctuating velocities of both phases is not yet available. For that reason, Koch (1990) first derived a theoretical expression for $\overline{u'_{si}u'_{fi}}$ in gas–particle flows of very high St_T and $Re_T<1$. Louge et al. (1991) subsequently extrapolated the Koch (1990) expression to turbulent gas–particle flows in which $Re_T>1$ Eq. (6).

$$\overline{u'_{fi}u'_{si}}=\beta\frac{4d_p}{\sqrt{\pi}\rho_s}\frac{(1-\upsilon)}{\upsilon}\frac{(U_{fz}-U_{sz})^2}{\sqrt{T}} \tag{6}$$

Wylie et al. (2003) followed up on the work of Koch (1990) by incorporating the fluid inertia effect on the particle fluctuation, and derived a description for $\overline{u'_{si}u'_{fi}}$ using their lattice Boltzmann simulation results. The detailed description of the closure model of Wylie et al. (2003), which is most applicable for flows of $St_T\gg1$ and $Re_T>1$, is provided in Table 4.

Bolio et al. (1995) reported that accurate predictions of the granular temperature, were obtained using the Louge et al. (1991) expression, particularly for high St_T flows ($St_T\geqslant1000$). The turbulent kinetic energy, however, was considerably underpredicted. Therefore, Bolio and Sinclair (1995) incorporated a new turbulence enhancement mechanism attributed to the particle wake formation ($\overline{E_W}$) to improve the model prediction. However, the particle wake formation is only existent in gas-particle flows, in the absence of particle rotation, for rapid flows of very massive particles ($d_p>500$ μm). With that in mind, an alternative

Table 4
Turbulence closure model of Wylie et al (2003).

$\beta\overline{u'_{fi}u'_{si}}=\frac{81\mu_f^2\upsilon(U_{fz}-U_{sz})^2}{\rho_s d_p^3\sqrt{\pi T}}R_S R_D^2$

$R_S=(\chi(1+3.5\upsilon^{0.5}+5.9\upsilon))^{-1}$	$\chi=\frac{1+2.5\upsilon+4.5094\upsilon^2+4.5154\upsilon^3}{[1-(\upsilon/0.6436)^3]^{3.0.6780}}$
$R_D=R_{D0}+K_{fb}Re_P\psi$	$R_{D0}=\frac{1+3/\sqrt{2}\upsilon^{0.5}+(135/64)\upsilon\ln\upsilon+17.14\upsilon}{1+0.681\upsilon-8.48\upsilon^2+8.16\upsilon^3}$
$K_{fb}=0.0336+0.106\upsilon+0.0116(1-\upsilon)^{-5}$	$(Re_P=\rho_f d_p\lvert U_f-U_s\rvert/\mu_f)$
$\psi=\left(1+\frac{2Re_T^2}{Re_P^2}-\frac{Re_T^4}{Re_P^4}\right)erf\left(\frac{Re_P}{\sqrt{2}Re_T}\right)+\sqrt{\frac{2}{\pi}}\frac{Re_T}{Re_P}\left(1+\frac{Re_T^2}{Re_P^2}\right)\exp\left(-\frac{Re_P^2}{2Re_T^2}\right)$	

closure model for $\overline{u'_{si}u'_{fi}}$ Eq. (7) was introduced by Sinclair and Mallo (1998).

$$\overline{u'_{si}u'_{fi}}=\sqrt{2k3T} \tag{7}$$

Using this closure model, Hadinoto and Curtis (2004) reported that reasonable predictions for both the granular temperature and turbulent kinetic energy were obtained for high St_T flows, though not yet quantitatively accurate. In this work, the impacts of employing the Louge et al. (1991), Wylie et al. (2003), and Sinclair and Mallo (1998) expressions on the model predictions for moderate St_T and low-Re flows are assessed.

3. Results and discussion

The two-phase flow CFD model predictions for the mean slip velocity, turbulent kinetic energy, and granular temperature are examined for the two experimental case studies detailed in Table 1. First, the effect of employing different drag correlations on the model predictive capability is investigated. Second, the CFD model predictive capability in the Re influence on the gas-phase turbulence modulation is examined (i) for the case where Re is varied by changing the mean superficial velocity and (ii) for the case where Re is varied by changing the pipe diameter. Unfortunately, only the CFD model predictions for (i) that can be compared with the trends observed in the experiment, as experimental data for (ii) are not yet available.

In this work, the analysis is based on the dimensionless velocity data that are normalized by the single-phase centerline gas mean velocity, U_0, to take into account the change in the single-phase mean velocity at different Re. The U_0 values vary from 8 to 18 m/s for the Re range investigated. The gas-phase turbulence intensity is defined as $\overline{u'_{fi}u'_{fi}}/U_0^2$,where $\overline{u'_{fi}u'_{fi}}=(\overline{u'_{fz}u'_{fz}}+2\overline{u'_{fr}u'_{fr}})$ assuming that the magnitude of the azimuthal and radial fluctuating velocities are equal. Similarly, the particle fluctuating intensity is defined as $\overline{u'_{si}u'_{si}}/U_0^2$ with $\overline{u'_{si}u'_{si}}=(\overline{u'_{sz}u'_{sz}}+2\overline{u'_{sr}u'_{sr}})$. The unladen flow predictions for the mean velocity and turbulent kinetic energy have been successfully validated by Hadinoto and Curtis (2004) and the simulation results have been verified to be grid-independent.

3.1. Selection of drag correlation for moderate St_T flows

The current investigation is conducted for gas-particle flows involving the cenospheres and glass bead particles at Re = 6000 and $m=0.4$, which represent moderate St_T and low-Re turbulent particle-laden flows. The St_T for the cenospheres and glass bead particles are 126 and 507, respectively (Table 1). The effects of employing the seven different drag correlations in Table 3 on the CFD model predictions are investigated. The model predictions, and their corresponding experimental data, of the mean slip velocity, turbulent kinetic energy, and granular temperature are displayed in Figs. 3–5, respectively.

The Sinclair and Mallo (1998) turbulence closure model is employed in all simulation runs to describe the $\overline{u'_{si}u'_{fi}}$ correlation.

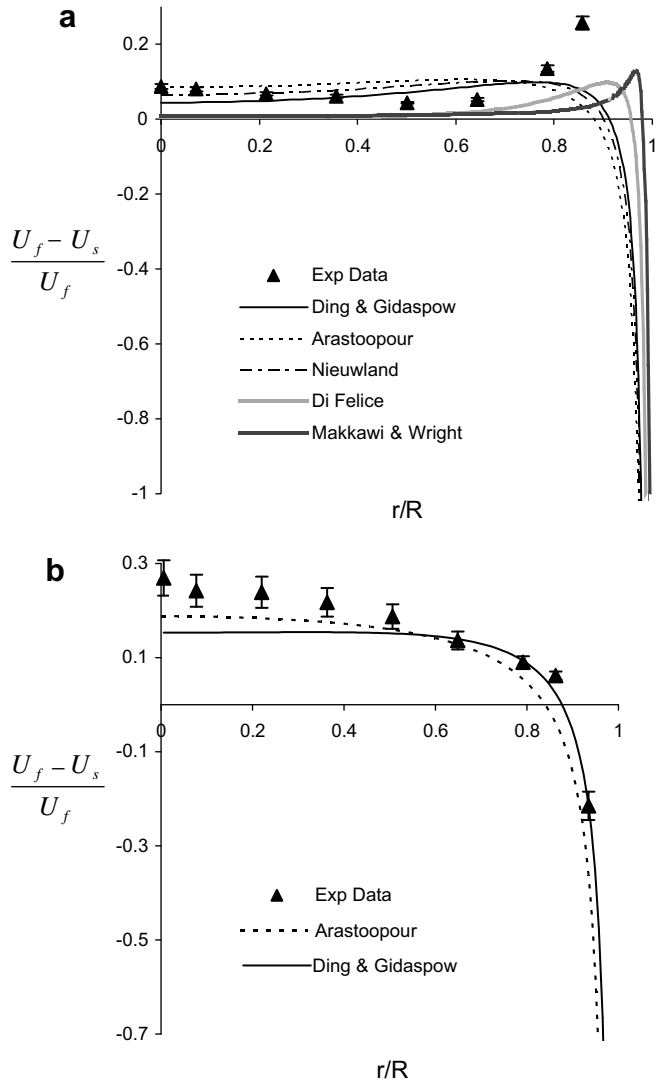

Fig. 3. The model predictions of the normalized mean slip velocity at Re = 6000 and m = 0.4. (a) Cenospheres and (b) glass beads.

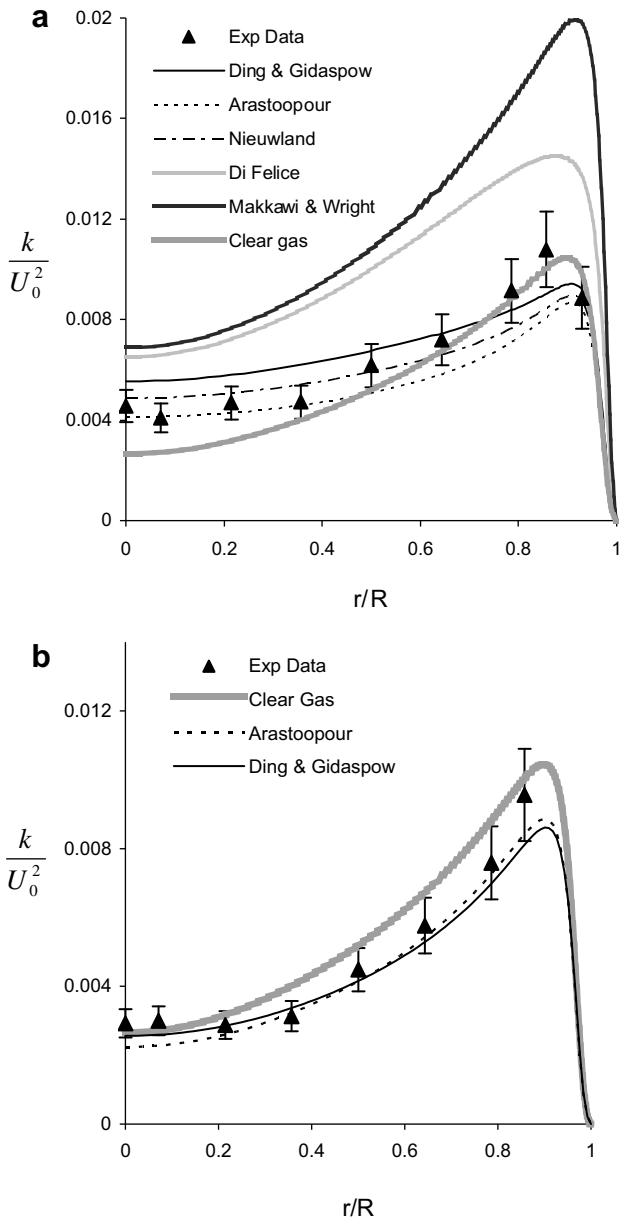

Fig. 4. The model predictions of the turbulent kinetic energy at Re = 6000 and m = 0.4. (a) Cenospheres and (b) glass beads.

When the Louge et al. (1991) closure model is employed in this gas-particle flow regime, the simulation fails to produce a converged solution. The failure is attributed to the turbulent kinetic energy prediction that rapidly approaches zero, as a result of an insufficient energy source term from the $\overline{u'_{si}u'_{fi}}$ correlation. Similarly, using the Wylie et al. (2003) closure model, the $\overline{u'_{si}u'_{fi}}$ correlation for these moderate St_T flows are considerably underestimated resulting in a failed convergence. The failure is attributed to the fact that Wylie et al. (2003) closure model was obtained from a lattice-Boltzmann simulation of very high St_T flows, where the influence of the hydrodynamic interactions on the particle fluctuating velocity between successive interparticle collisions was minimal, which is not the case in the present case studies.

The simulation results suggest that the correlations of Ding and Gidaspow (1990), Arastoopour et al. (1990), and Nieuwland et al. (1994) yield qualitatively similar predictions at the mean and fluctuating velocity levels (Figs. 3a, 4a, and 5a). The model predictions obtained using the Difelice (1994) and Makkawi and Wright (2003) correlations are qualitatively comparable with each other, but notably differ from the previous three correlations. Simulations using the Hill et al. (2001) correlation, on the other hand, vastly overpredict the granular temperature in this gas-particle flow regime. Hence, the results are not presented here. Importantly, the inclusion of the particle fluctuating velocity into the slip velocity calculation (Zhang and Reese, 2003b) leads to model predictions that resemble the ones obtained using the time-averaged (or mean) value for the slip velocity. In other words, the effect of incorporating the particle fluctuating velocity into the drag formulation on the mean and fluctuating velocity predictions is insignificant. Hence, the slip velocity in this work is calculated using the mean value.

3.1.1. Mean slip velocity predictions

For the cenospheres particles ($St_T \sim 100$), the model predictions of the mean slipvelocity are quantitatively comparable with the experimental results for all the drag correlations investigated (Fig. 3a). However, only simulations employing the correlations of the Difelice (1994) and Makkawi and Wright (2003) are capable of capturing the positive peak in the slip velocity near the pipe

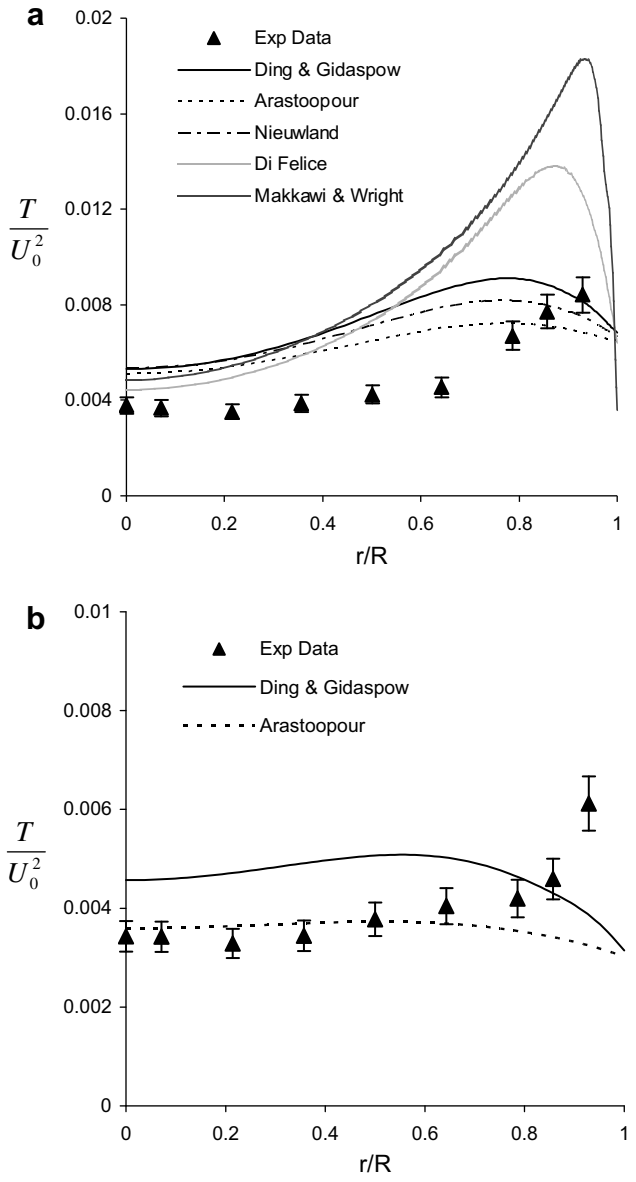

Fig. 5. The model predictions of the granular temperature at Re = 6000 and m = 0.4. (a) Cenospheres and (b) glass beads.

wall. Therefore, the Difelice (1994) and Makkawi and Wright (2003) correlations are superior in that regard.

For the glass bead particles ($St_T \sim 500$), simulations employing any of the five correlations are all capable of accurately predicting the mean slip velocity throughout the pipe radius. The best model predictions are obtained by employing the Ding and Gidaspow (1990) and Arastoopour et al. (1990) correlations (Fig. 3b). The model predictions using the other three drag correlations are not shown for clarity. Therefore, the results suggest that the impact of selecting different drag correlations is minimal at the mean velocity level, particularly for flows of moderate to high St_T particles.

3.1.2. Turbulent kinetic energy predictions

Next, the impact of employing different drag correlations at the fluctuating velocity level is investigated. For the cenospheres particles, the model predictions of the gas-phase turbulent kinetic energy obtained using the Ding and Gidaspow (1990, Arastoopour et al., 1990, and Nieuwland et al. (1994) correlations are comparable with the experimental results (Fig. 4a). On the other hand, the predictions obtained using the Difelice (1994) and Makkawi and Wright (2003) correlations vastly overpredict the experimental results. Significantly, the simulations are capable of capturing the gas-phase turbulence enhancement with respect to the unladen flow in the pipe core at Re = 6000 for the cenospheres particles. Hence, the use of the Sinclair and Mallo (1998) closure model in this gas-particle flow regime has been justified.

For the glass bead particles, simulations employing the Ding and Gidaspow (1990) and Arastoopour et al. (1990) correlations can accurately predict the gas-phase turbulent kinetic energy (Fig. 4b). Similar to the simulation results of the cenospheres particles, simulations employing the Difelice (1994) and Makkawi and Wright (2003) correlations vastly overpredict the turbulent kinetic energy (not shown for a better clarity). Importantly, the applicability of the Sinclair and Mallo (1998) closure model in this gas-particle flow regime has been again reaffirmed.

3.1.3. Granular temperature predictions

Lastly, the impact of employing different drag correlations on the granular temperature predictions is investigated. For both the cenospheres and glass bead particles, the simulations overpredict the experimental results in the pipe core for all the drag correlations investigated, except for the Arastoopour et al. (1990) correlation. The degree of overprediction for the glass bead particles, however, is lower than that for the cenospheres particles. This is attributed to the fact that the kinetic theory of granular flow description of the particle-phase stresses is most applicable for rapid flows of high St_T particles. Importantly, the degree of the overprediction is found to be dependent on the choice of the drag correlation. Similar to the turbulent kinetic energy results, simulations employing the Difelice (1994) and Makkawi and Wright (2003) correlations vastly overpredict the experimental results of the granular temperature for both the cenospheres and glass bead particles. Also similar, the best quantitative predictions of the granular temperature are obtained by employing the Ding and Gidaspow (1990) and Arastoopour et al. (1990) correlations.

The authors, however, acknowledge that the model predictions of the granular temperature still leave much room for improvement. As the resulting granular temperature in the pipe core is the product of the fluctuating energy transfer from the pipe wall, more accurate values of e_w and σ, particularly for the cenospheres particles, need to be acquired. Moreover, the $\overline{u_{si}'u_{fi}'}$ correlation, which is currently treated as equal in both the granular temperature and turbulent kinetic energy balances, though not physically correct, may require different closure models for the continuous and dispersed phases. Therefore, the use of DNS coupled with discrete element method, or lattice Boltzmann simulation is required for this purpose. The current gas-particle flow data at lower Re, which fall within the DNS range, can be utilized to validate the simulation results.

A summary of the model predictions for the mean slip velocity, turbulent kinetic energy, and the granular temperature for the cenospheres and glass bead particles is presented in Tables 5a and 5b, respectively. Due to the deficiencies in their turbulent kinetic energy and granular temperature predictions, this work concludes that the Difelice (1994) and Makkawi and Wright (2003) correlations are not suitable to describe the fluctuating drag force for this gas-particle flow regime. This is despite the fact that they are the only drag correlations that can accurately capture the mean slip velocity profile of the cenospheres particles. Among the remaining three drag correlations, which are qualitatively comparable in their predictions, the simulations employing the Arastoopour et al., 1990 correlation yield the best quantitative prediction, though not yet accurate, at the fluctuating velocity level. Therefore, the

Table 5a
Summary of the model predictions for the cenospheres particles.

Drag correlation[b]	$\frac{U_f-U_s}{U_f}$[a]		$\frac{k}{U_0^2}$[a]		$\frac{T}{U_0^2}$[a]	
	Pipe core	Pipe wall	Pipe core	Pipe wall	Pipe core	Pipe wall
Ding and Gidaspow (1990)	o	Under	o	o	Over	o
Arastoopour et al (1990)	o	Under	o	o	Over	o
Nieuwland et al (1994)	o	Under	o	o	Over	o
Difelice (1994)	o	o	Over	Over	Over	Over
Makkawi and Wright (2003)	o	o	Over	Over	Over	Over

[a] Over, overprediction; Under, underprediction; o, accurate within the experimental uncertainty.
[b] Simulation results using the Sinclair and Mallo (1998) turbulence closure model at Re = 6000.

Table 5b
Summary of the model predictions for the glass bead particles.

Drag correlation[a]	$\frac{U_f-U_s}{U_f}$[b]		$\frac{k}{U_0^2}$[b]		$\frac{T}{U_0^2}$[b]	
	Pipe core	Pipe wall	Pipe core	Pipe wall	Pipe core	Pipe wall
Ding and Gidaspow (1990)	o	o	o	o	Over	Under
Arastoopour et al (1990)	o	o	o	o	o	Under
Nieuwland et al (1994)	o	o	o	o	Over	Under
Difelice (1994)	o	o	Over	Over	Over	Over
Makkawi and Wright (2003)	o	o	Over	Over	Over	Over

[a] Simulation results using the Sinclair and Mallo (1998) turbulence closure model at Re = 6000.
[b] Over, overprediction; Under, underprediction; o, accurate within the experimental uncertainty.

Arastoopour et al., (1990) correlation is employed in the subsequent simulations.

3.2. Model prediction: Re influence on the gas-phase turbulence modulation

3.2.1. Re variation by changing gas-phase mean superficial velocity

Next, the CFD model predictive capability in capturing the Re dependence of the gas-phase turbulence modulation is investigated using the Arastoopour et al., 1990 drag correlation. The current investigation is conducted for the two case studies in Table 1. The model predictions for the turbulent kinetic energy in the presence of the cenospheres (Case 2) and glass bead (Case 1) particles are displayed in Figs. 6 and 7, respectively. For both the cenospheres and glass bead particles, the simulations predict a decrease in the normalized turbulent kinetic energy in the pipe core with increasing Re, which is similar to the trend in the unladen flow (Table 6). The predicted decrease in the turbulent kinetic energy with Re, however, is more substantial for the cenospheres particles than that of the glass bead particles. Importantly, the model predictions for the trends in the gas-phase turbulence modulation as a function of Re agree with the experimental observation for the cenospheres particles, but not for the glass bead particles. A more detailed discussion is provided below.

3.2.1.1. Turbulent kinetic energy: cenospheres particles. In the presence of the cenospheres particles, the simulations consistently predict that the gas-phase turbulence intensity is enhanced in the pipe core with respect to the unladen flow, and is slightly attenuated elsewhere in the pipe for all the Re investigated (Figs. 4a and 6). In contrast, the experimental results indicate that the turbulence enhancement in the pipe core occurs only at Re = 6000, whereas the gas-phase turbulence intensity at higher Re is comparable to that of the unladen flow. The discrepancy between the simulation and experimental results is attributed to the fact that the predicted decrease in the turbulent kinetic energy in the pipe core, as Re is raised from 6000 to 10,000, is notably less than the actual decrease reported in the experiment (Table 6).

A closer look at the turbulent kinetic energy budget reaffirms the fact that the energy budget near the pipe wall, where the mean slip velocity and gas-phase radial velocity gradient are significant, determines the resulting turbulence in the pipe core, and not vice versa. Therefore, accurate predictions of the mean slip velocity and its Re dependence near the pipe wall are crucial for the CFD model to be able to capture the Re influence on the gas-phase turbulence intensity in the pipe core. For the cenospheres particles, unfortunately, the simulations employing the Arastoopour et al. (1990)

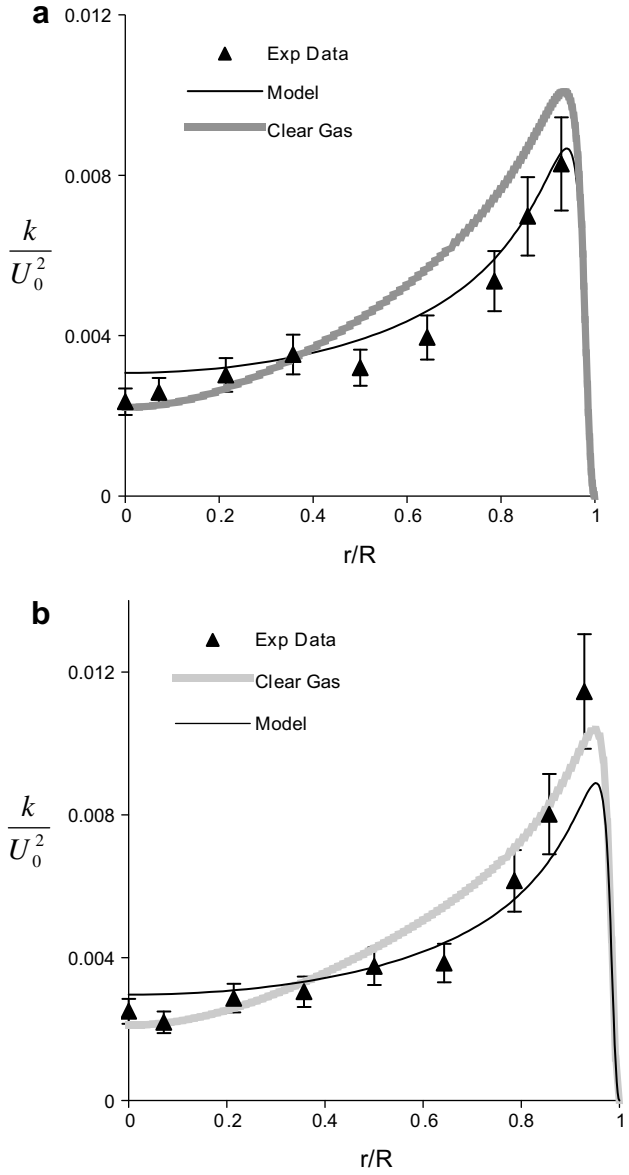

Fig. 6. The model predictions of the turbulent kinetic energy in the presence of the cenospheres at $m = 0.4$. (a) Re = 10,000 and (b) Re = 13,000.

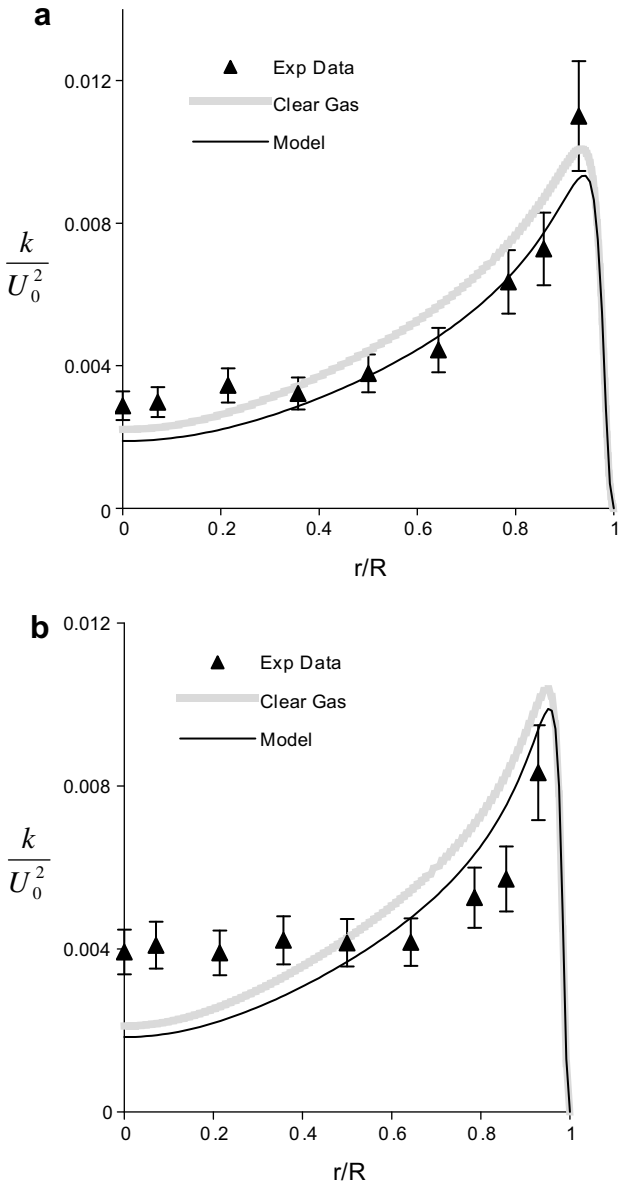

Fig. 7. The model predictions of the turbulent kinetic energy in the presence of the glass beads at $m = 0.4$. (a) Re = 10,000 and (b) Re = 13,000.

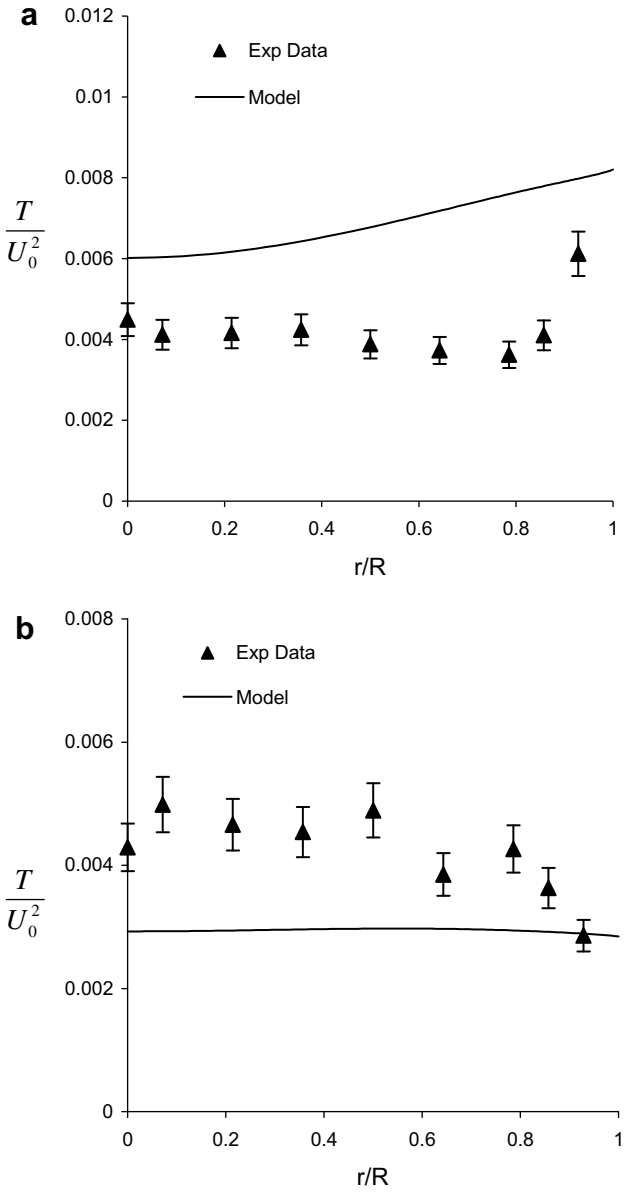

Fig. 8. The model predictions of the granular temperature at $m = 0.4$ and Re = 13,000 for (a) cenospheres and (b) glass beads.

Table 6
Gas-phase turbulent kinetic energy at the pipe centerline.

Re	k/U_o^2				
	Unladen Flow	Case 1: Model	Case 1: Experiment	Case 2: Model	Case 2: Experiment
6000	0.0027	0.0022	0.0029	0.0041	0.0046
10,000	0.0022	0.0019	0.0041	0.0031	0.0024
13,000	0.0021	0.0018	0.0040	0.0030	0.0025

drag correlation, which yield the best quantitative predictions at the fluctuating velocity level, still fail to accurately predict the mean slip velocity near the pipe wall at Re = 6000 (Figs. 3a). Subsequent simulations at Re = 10,000 and 13,000 (not shown) also fail to accurately capture the mean slip velocity near the pipe wall.

Therefore, the lack of ability of the CFD model in capturing the Re dependence of the gas-phase turbulence modulation in the presence of the cenospheres particles is not unexpected, as the CFD model is still not capable of accurately predicting the mean slip velocity near the pipe wall. Despite this lack of ability, however, the model on the whole is still capable of yielding good predictions for the turbulent kinetic energy. As a result, good predictions for the pressure drop that are of significant importance in a pneumatic conveyor design can be expected.

3.2.1.2. Turbulent kinetic energy: glass bead particles. In the presence of the glass bead particles, the simulations consistently predict slight turbulence attenuation throughout the pipe radius for all the Re investigated (Figs. 4b and 7). The simulation results therefore are in contrast to the experimental results, where the turbulence enhancement at $Re \geqslant 13,000$ is observed in the pipe core. Furthermore, the predicted turbulent kinetic energy in the pipe core, which agrees with the experimental result at Re = 6000, notably deviates from the experimental results at higher Re (Fig. 7). Consequently, the pressure drop predictions are anticipated to deteriorate at higher Re as well. As opposed to the cenospheres particles, however, the mean slip velocity near the pipe wall for

the glass bead particles can accurately be predicted by the model (Fig. 3b). Therefore, the lack of ability of the CFD model in accurately predicting the turbulent kinetic energy is not due to the inaccurate prediction of the mean slip velocity, but more likely due to the incomplete descriptions of the fluctuating drag force. Employing a different drag correlation (i.e. Ding and Gidaspow, 1990) yields similar predictions for the turbulent kinetic energy. Therefore, improved drag correlations and turbulence closure models that take into account the increased microscale fluid inertia and the formation of mesoscale structures at higher Re are needed.

3.2.1.3. Granular temperature: cenospheres and glass bead particles. Next, the Re influence on the granular temperature predictions, which reflect the particle spatial distribution, is examined. The CFD model, which overpredicts the granular temperature of the cenospheres particles in the pipe core at Re = 6000 (Fig. 5a), yields a similar overprediction throughout the pipe radius at Re = 13,000 (Fig. 8a). Hence, the overprediction of the granular temperature is not limited to only moderate St_T and low-Re turbulent flows as previously thought. Nevertheless, the granular temperature prediction near the pipe wall at Re = 13,000 exhibit an improvement compared to that at Re = 6000. The simulation result at Re = 13000 is able to predict that the highest granular temperature is very near the pipe wall, as observed in the experiment, whereas the prediction at Re = 6000 fails to do so. The results indicate the estimated values for the e_w and σ parameters are more suitable for higher Re flows.

For the glass bead particles, the CFD model significantly underpredicts the granular temperature in the pipe core at Re = 13,000 (Fig. 8b), whereas the model prediction at Re = 6000 yields a reasonable result (Fig. 5b). Significantly, the simulation result fails to capture the change in the granular temperature profile with Re that is observed in the experiment. At Re = 6000, the experimental results indicate that the granular temperature peaks near the pipe wall, as opposed to the peak that is observed near the pipe center at Re = 13,000. The simulation results of the cenospheres and glass bead particles at different Re reiterate the need to develop

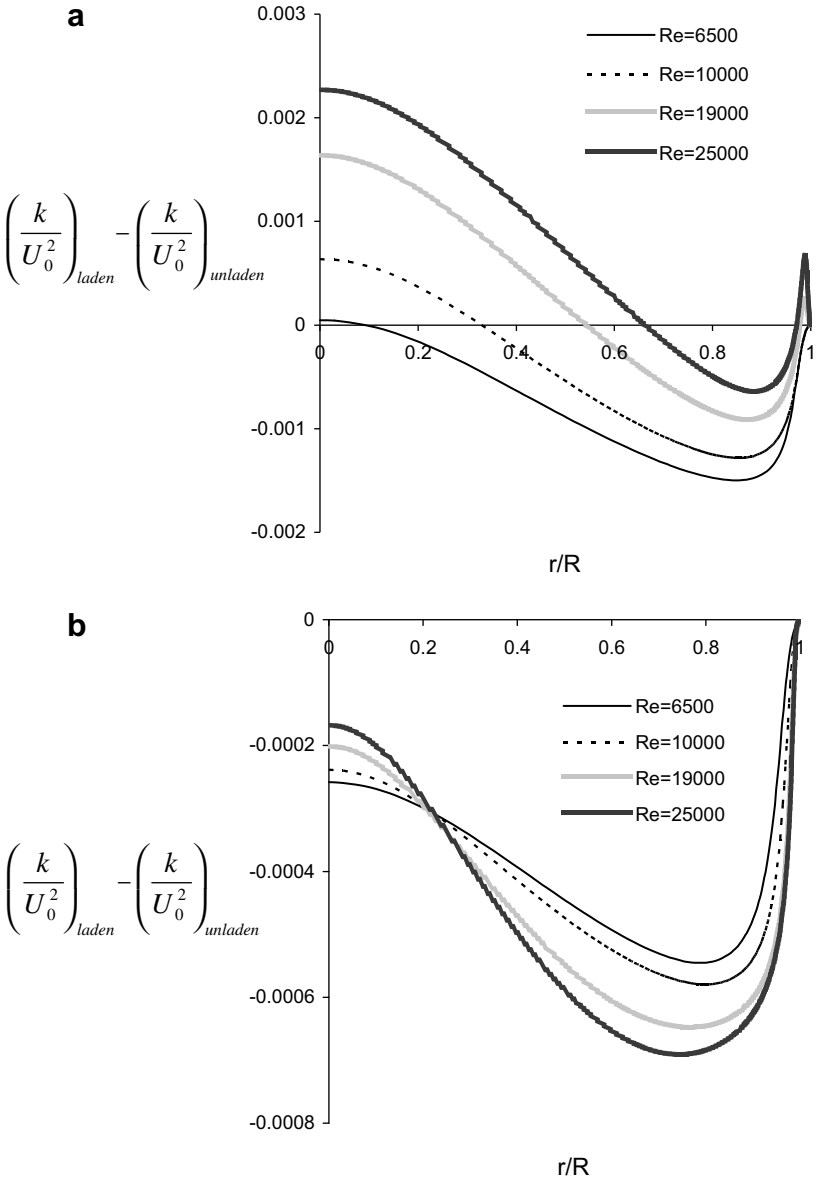

Fig. 9. The change in the gas-phase turbulence intensity as a function of the Re in the presence of (a) cenospheres and (b) glass beads.

an improved correlation for the $\overline{u'_{si}u'_{fi}}$ correlation that is applicable to moderate St_T flows and finite fluid inertia.

3.2.2. Re variation by changing pipe diameter

The simulation results presented in Section 3.2.1 consistently predict a decrease in the gas-phase turbulence intensity with increasing Re in the presence of non-massive particles ($\leqslant$ 200 μm), which contradicts the experimental observation for the glass bead particles. Therefore, this study aims to examine whether the present CFD model is actually equipped to predict gas-phase turbulence enhancement at high Re. For that purpose, the Re influence on the gas-phase turbulence modulation is simulated for the case where Re is varied by changing the flow length scale (i.e. pipe radius), instead of the velocity scale. The Re investigated are 6500, 10,000, 19,000, and 25,000, which correspond to pipe radius of R, 1.25 * R, 2.8 * R, and 3.6 * R, respectively. The simulations are conducted for both the cenospheres and glass bead particles at m = 0.4.In the present simulation, the mean gas velocity at the pipe center ($U_{f\cdot\text{center}}$) is maintained constant while the pipe radius is varied. The simulation results for the change in the gas-phase turbulent kinetic energy as a function of Re are presented in Fig. 9. The model parameters and flow conditions are summarized in Table 7.

In the presence of the cenospheres particles, the gas-phase turbulence intensity in the pipe core at Re = 6500 is initially predicted to be comparable with the unladen flow at the same Re (Fig. 9a). The predicted turbulence intensity, however, increases with Re, as indicated by the value of the change in the turbulent kinetic energy that becomes more positive at higher Re. Hence, in contrast to the previous simulation results (Section 3.2.1), the CFD model predicts an enhancement of the gas-phase turbulence intensity at higher Re in the presence of the cenospheres particles. For the glass bead particles, the CFD model predicts a decrease in the gas-phase turbulence intensity away from the pipe core with increasing Re, where on the other hand a turbulence enhancement at higher Re is predicted in the pipe core (Fig. 9b).

The current simulation result of the cenospheres and glass bead particles suggests that the CFD model can predict gas-phase turbulence enhancement at high Re in the presence of non-massive particles. For gas–particle flows involving non-massive particles ($\text{Re}_P \leqslant 400$), the wake formation mechanism that enhances the turbulence is excluded from the turbulent kinetic energy formulation ($\overline{E_W}$ in Eq. (3)). Therefore, the current simulation result suggests that it is possible to have an enhancement of the gas-phase turbulence intensity in the absence of the wake formation for non-massive particles, in contrast to what is previously thought. Consequently, the current simulation result supports our hypothesis that the gas-phase turbulence enhancement at high Re for these non-massive particles is likely caused by physical mechanisms other than the particle wake formation, such as an altered turbulence production, mesoscale structure formation, and change in particle concentration profile. For this purpose, the experimental works to validate the current simulation results and to identify the turbulence modulation mechanism are currently being pursued in our research group.

Table 7
Summary of the model parameters for Cases A and B.

Particle	Re	$U_{f\cdot\text{center}}$ (m/s)	e_s	e_{ws}	e_f	e_{wf}	σ
Case A: Glass beads, m = 0.4	6500	18.2	0.94	0.15	0.85	0.13	0.008
	10,000				0.90	0.14	
	19,000				0.94	0.15	
	25,000				0.94	0.15	
Case B: Cenospheres, m = 0.4	6500	17.3	0.94	0.94	0.80	0.80	0.008
	10,000				0.85	0.85	
	19,000				0.90	0.90	
	25,000				0.94	0.94	

4. Conclusions

The present work examines the CFD model predictive capability in capturing the trend in the gas-phase turbulence modulation as a function of Re. The model predictive capability in simulating moderate St_T and low Re turbulent particle-laden flows is also evaluated. Drag correlation and turbulence closure model that yield the best predictions at both the mean and fluctuating velocity levels for this gas–particle flow regime have been identified. Importantly, the present work concludes that the current state of the two-phase flow CFD model is not yet capable of simulating the turbulence enhancement phenomenon at high Re for the case where Re is varied by changing the velocity scale. Improved turbulence closure models and drag correlations that take into account the increased microscale fluid inertia at high Re need to be incorporated to improve the model predictive capability. Nevertheless, the CFD model is capable of simulating gas-particle flow systems at both the mean and fluctuating velocity levels for flows where the gas-phase turbulence enhancement at high Re is not evident.

Acknowledgements

Financial supports from Nanyang Technological University's Start-up Grant (Grant No. SUG 8/07) and American Chemical Society Petroleum Research Fund (Grant No. ACS-PFR#35117-AC9) are gratefully acknowledged.

References

Agrawal, K., Loezos, P.N., Syamlal, M., Sundaresan, S., 2001. The role of meso-scale structures in rapid gas-solid flows. J. Fluid Mech. 445, 151–185.
Arastoopour, H., Pakdel, P., Adewumi, M., 1990. Hydrodynamic analysis of dilute gas solids flow in a vertical pipe. Powder Technol. 62, 163–170.
Bolio, E.J., Sinclair, J.L., 1995. Gas turbulence modulation in the pneumatic conveying of massive particles in vertical tubes. Int. J. Multiphase Flow 21 (6), 985–1001.
Bolio, E.J., Yasuna, J.A., Sinclair, J.L., 1995. Dilute turbulent gas–solid flow in risers with particle–particle interactions. AIChE J. 41 (6), 1375–1388.
Davidson, D., 2001. The enterprise-wide application of CFD in the chemicals industry. In: Proc. of the 6th World Congress of Chem. Eng., Melbourne, Australia.
Difelice, R., 1994. The voidage function for fluid particle interaction systems. Int. J. Multiphase Flow 20, 153–159.
Ding, J., Gidaspow, D., 1990. A bubbling fluidization model using kinetic-theory of granular flow. AIChE J. 36, 523–538.
Du, W., Bao, X.J., Xu, J., Wei, W.S., 2006. Computational fluid dynamics (CFD) modeling of spouted bed: assessment of drag coefficient correlations. Chem. Eng. Sci. 61, 1401–1420.
Elghobashi, S., 1994. On predicting particle-laden turbulent flows. Appl. Sci. Res. 52, 309–329.
Goldsmith, W., 1960. Impacts: The Theory and Physical Behavior of Colliding Solids. Edwards Arnold Publisher, London.
Gondret, P., Lance, M., Petit, L., 2002. Bouncing motion of spherical particles in fluids. Phys. Fluids 14, 643–652.
Hadinoto, K., 2004. Experimental Investigation and CFD Modeling of Interstitial Fluid Effect in Fluid–Particle Flow with Particle–Particle Collisions. Ph.D. Thesis, Purdue University, West Lafayette, IN.
Hadinoto, K., Curtis, J.S., 2004. Effect of interstitial fluid on particle–particle interactions in kinetic theory approach of dilute turbulent fluid–particle flow. Ind. Eng. Chem. Res. 43, 3604–3615.
Hadinoto, K., Jones, E.N., Yurteri, C., Curtis, J.S., 2005. Reynolds number dependence of gas-phase turbulence in gas-particle flows. Int. J. Multiphase Flow 31, 416–434.
Henthorn, K.H., Park, K., Curtis, J.S., 2005. Measurement and prediction of pressure drop in pneumatic conveying: effect of particle characteristics, mass loading, and Reynolds number. Ind. Eng. Chem. Res. 44, 5090–5098.
Hetsroni, G., 1989. Particles turbulence interaction. Int. J. Multiphase Flow 15, 735–746.
Hill, R.J., Koch, D.L., Ladd, A.J.C., 2001. The first effects of fluid inertia on flows in ordered and random arrays of spheres. J. Fluid Mech. 448, 213–241.
Johnson, P.C., Jackson, R., 1987. Frictional collisional constitutive relations for antigranulocytes-materials, with application to plane shearing. J. Fluid Mech. 176, 67–93.

Kiml, R., Magda, A., Mochizuki, S., Murata, A., 2004. Rib-induced secondary flow effects on local circumferential heat transfer distribution inside a circular rib-roughened tube. Int. J. Heat Mass Transfer 47, 1403–1412.

Koch, D.L., 1990. Kinetic-theory for a monodisperse gas–solid suspension. Phys. Fluids: A Fluid Dyn. 2, 1711–1723.

Lee, S.L., Durst, F., 1982. On the motion of particles in turbulent duct flows. Int. J. Multiphase Flow 8, 125–146.

Louge, M.Y., Mastorakos, E., Jenkins, J.T., 1991. The role of particle collisions in pneumatic transport. J. Fluid Mech. 231, 345–359.

Mabrouk, R., Chaouki, J., Guy, C., 2007. Effective drag coefficient investigation in the acceleration zone of an upward gas–solid flow. Chem. Eng. Sci. 62, 318–327.

Makkawi, Y.T., Wright, P.C., 2003. The voidage function and effective drag force for fluidized beds. Chem. Eng. Sci. 58, 2035–2051.

Marcus, R., Leung, L., Klinzing, G., Rizk, F., 1990. Pneumatic Conveying of Solids. Chapman and Hall, London.

Myong, H.K., Kasagi, N., 1990. A new approach to the improvement of kappa-epsilon turbulence model for wall-bounded shear flows. JSME Int. J. I-Fluids Eng. Heat Transfer Power Combust. Thermophys. Properties 33, 63–72.

Nieuwland, J.J., Huizenga, P., Kuipers, J.A.M., van Swaaij, W.P.M., 1994. Hydrodynamic modelling of circulating fluidised beds. Chem. Eng. Sci. 49, 5803–5811.

Patankar, S., 1980. Numerical Heat Transfer and Fluid Flow. Hemisphere Publishing Co., New York.

Richardson, J., Zaki, W., 1954. Sedimentation and fluidization: Part I. Trans. Inst. Chem. Eng. 32, 35–53.

Sinclair, J.L., Mallo, T., 1998. Describing particle turbulence interaction in a two-fluid modeling framework. In: Proceedings of FEDSM'98: ASME Fluids Engineering Division Summer Meeting 4, pp. 7–14.

Tsuji, Y., Morikawa, Y., Shiomi, H., 1984. Ldv measurements of an air solid. 2. Phase Flow in a vertical pipe. J. Fluid Mech. 139, 417–434.

Vaishali, S., Roy, S., Bhusarapu, S., Al-Dahhan, M.H., Dudukovic, M.P., 2007. Numerical simulation of gas–solid dynamics in a circulating fluidized-bed riser with Geldart group B particles. Ind. Eng. Chem. Res. 46, 8620–8628.

Vasquez, N., Jacob, K., Cocco, R., Dhodapkar, S., Klinzing, G.E., 2008. Visual analysis of particle bouncing and its effect on pressure drop in dilute phase pneumatic conveying. Powder Technol. 179, 170–175.

Wen, C., Yu, Y., 1966. Mechanics of fluidization. Chem. Eng. Prog. Symp. Series 62, 100–111.

Wylie, J.J., Koch, D.L., Ladd, A.J.C., 2003. Rheology of suspensions with high particle inertia and moderate fluid inertia. J. Fluid Mech. 480, 95–118.

Yasuna, J.A., Moyer, H.R., Elliott, S., Sinclair, J.L., 1995. Quantitative predictions of gas–particle flow in a vertical pipe with particle–particle interactions. Powder Technol. 84, 23–34.

Zhang, Y.H., Reese, J.M., 2003a. Gas turbulence modulation in a two-fluid model for gas–solid flows. AIChE J. 49, 3048–3065.

Zhang, Y.H., Reese, J.M., 2003b. The drag force in two-fluid models of gas–solid flows. Chem. Eng. Sci. 58, 1641–1644.